A UNITED STATES DEPARTMENT OF COMMERCE PUBLICATION

NOAA Technical Memorandum ERL SEL-21

U.S. DEPARTMENT OF COMMERCE
NATIONAL OCEANIC AND ATMOSPHERIC ADMINISTRATION
Environmental Research Laboratories

Observations of Proton Spectra ($1.0 \leq E_p \leq 300$ keV) and Pitch Angle Distributions at the Plasmapause

D.J. WILLIAMS
T.A. FRITZ
A. KONRADI

Space Environment Laboratory
BOULDER, COLORADO
June 1972

ENVIRONMENTAL RESEARCH LABORATORIES

SPACE ENVIRONMENT LABORATORY

NATIONAL OCEANIC AND ATMOSPHERIC ADMINISTRATION

BOULDER, COLORADO

U.S. DEPARTMENT OF COMMERCE
National Oceanic and Atmospheric Administration
Environmental Research Laboratories

NOAA Technical Memorandum ERL SEL-21

OBSERVATIONS OF PROTON SPECTRA ($1.0 \leq E_p \leq 300$ keV) AND PITCH ANGLE DISTRIBUTIONS AT THE PLASMAPAUSE

D. J. Williams
T. A. Fritz

Space Environment Laboratory

A. Konradi

Manned Spacecraft Center
National Aeronautics and Space Administration
Houston, Texas

Space Environment Laboratory
Boulder, Colorado
June 1972

OBSERVATIONS OF PROTON SPECTRA ($1.0 \leq E_p \leq 300$ keV) AND PITCH ANGLE DISTRIBUTIONS AT THE PLASMAPAUSE

D. J. Williams, T. A. Fritz, and A. Konradi

Detailed proton spectral and pitch angle distribution observations have been obtained from instrumentation flown aboard the NASA Small Scientific Satellite, S^3-A (Explorer 45). S^3 was launched from Kenya, Africa, into an elliptical orbit having an apogee of 5.24 R_E, a perigee of 220 km, an inclination of 3.5°, and a period of 7.82 hours. Data used in this initial report are from two proton detectors and a three axis fluxgate magnetometer. Data from the magnetometer are used to routinely display the particle data as a function of local pitch angle. The low energy proton instrument consists of an electrostatic analyzer-channeltron configuration measuring proton energies from 0.8 keV to 28 keV in 16 energy intervals. The high energy proton detector is a telescope detector system consisting of two surface barrier solid state detectors behind a 2.2 kilogauss magnet used to sweep out electrons of energy less than 300 keV. Electrons of energy > 300 keV are detected via the coincidence mode of the telescope. This latter instrument measures protons from 24 keV to 300 keV in six intervals. All pre-flight and in-flight calibrations indicate completely nominal operation. The satellite spin axis was placed in the orbital plane, and all

pitch angle distributions are obtained by sectoring the spin cycle into a number of samples. For the data reported herein, 32 samples per spin period (8.451 seconds) were obtained. See Longanecker and Hoffman (1972) for a more detailed description of the satellite and instrumentation.

The data of interest are from S^3 orbit 99 in-bound occurring on December 17, 1971, some 8 hours prior to the sudden commencement of a magnetic storm occurring on that date. The magnetic conditions at the time are shown in Cahill (1972) where moderate magnetic activity (30-40 γ) is present from apogee to L $\sim$ 3 on orbit 99. Figure 1 shows proton intensities in the energy range 24.3 to 35.1 keV as a function of altitude. Data are shown for two equatorial pitch angles, 90° and 45°. The solid vertical bar at the top of the figure indicates the point at which the S^3 electric field detector comes out of saturation and gives a rough estimate as to the location of the high density region of the plasmapause (Maynard and Cauffman, 1972). Three features to note in figure 1 are:

1. The high altitude (L > 4.0 earth radii) region of this particle distribution displays a relatively normal pitch angle distribution in that the intensity versus pitch angle plots peak at local pitch angles of 90°. The magnetic latitude of S^3 at this time is $\sim$12°. The data indicate that at these

higher altitudes the pitch angle distributions display a general form of $\sin^n\alpha$ with n varying from 1/3 - 2 depending on spatial location and energy. Variations from this form are often seen, especially at small pitch angles, but will not be discussed here.

2. At the steep radial gradient on the inner edge of the proton distribution the pitch angle distributions go over into a non-normal mode displaying strong off-equatorial peaking. This is evidenced by the fact that many more particles are observed at a pitch angle of 45° than at 90°.
3. The region of the large radial gradient corresponds well with the plasmapause location as measured by the electric field detector.

We have studied the evolution of proton pitch angle distributions for all energies measured throughout the spatial regions shown in figure 1. A sample of this evolution is presented in figure 2. Here the proton intensity is shown as a function of local pitch angle for three energy bands situated in the heart of the ring current distribution. Pitch angle distributions are shown from the high altitude "normal" portion of the particle distribution on into the gradient region shown in figure 1. We see that as the altitude decreases, the two high energy bands lose particles at all pitch angles. However, particles mirroring in the near equatorial

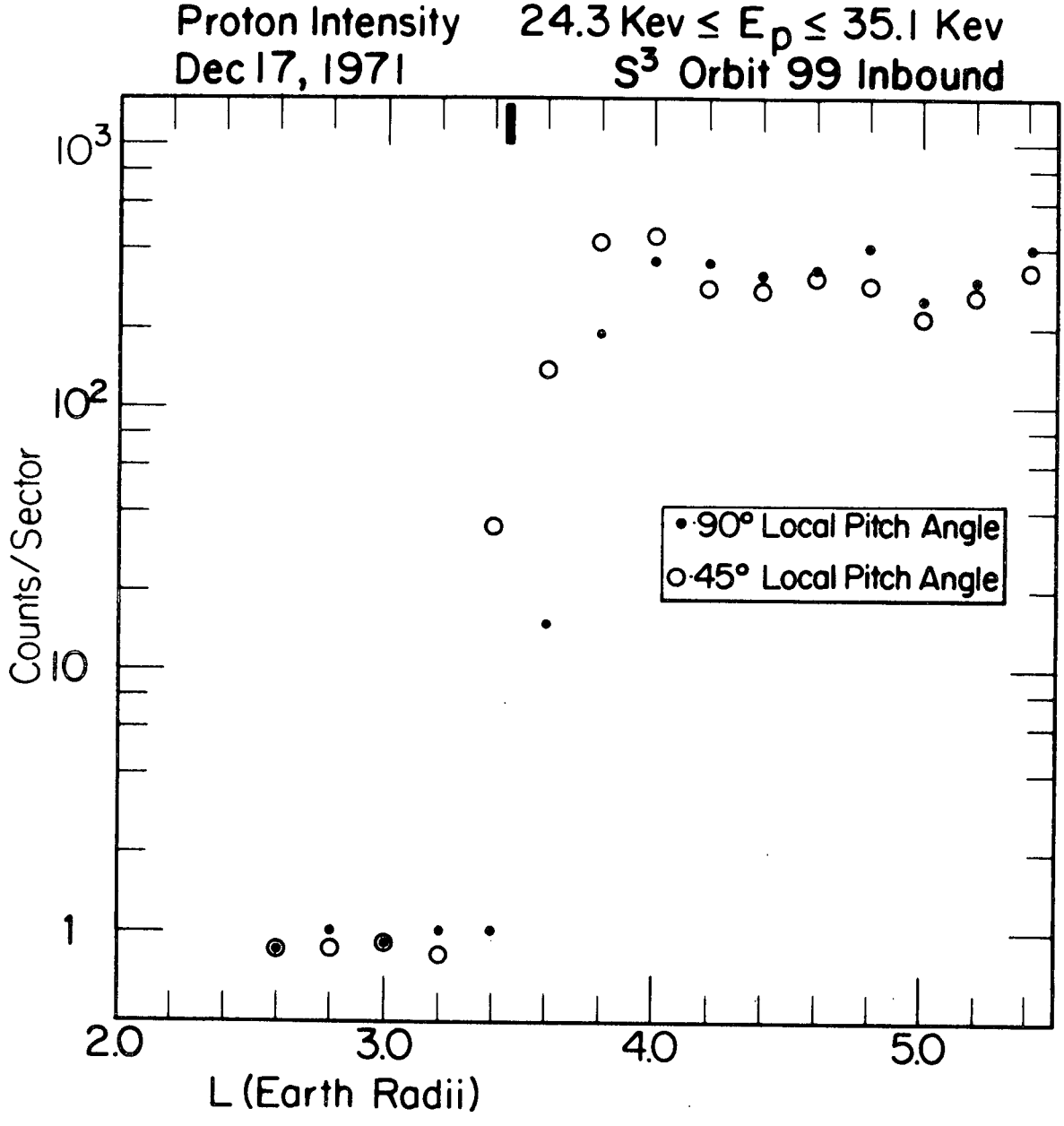

Figure 1. Proton intensity as a function of altitude. Sector = 0.264 seconds. Solid vertical bar at L = 3.45 is where DC electric field detector comes out of saturation, thereby providing indication of plasmapause (Maynard and Cauffman, 1972).

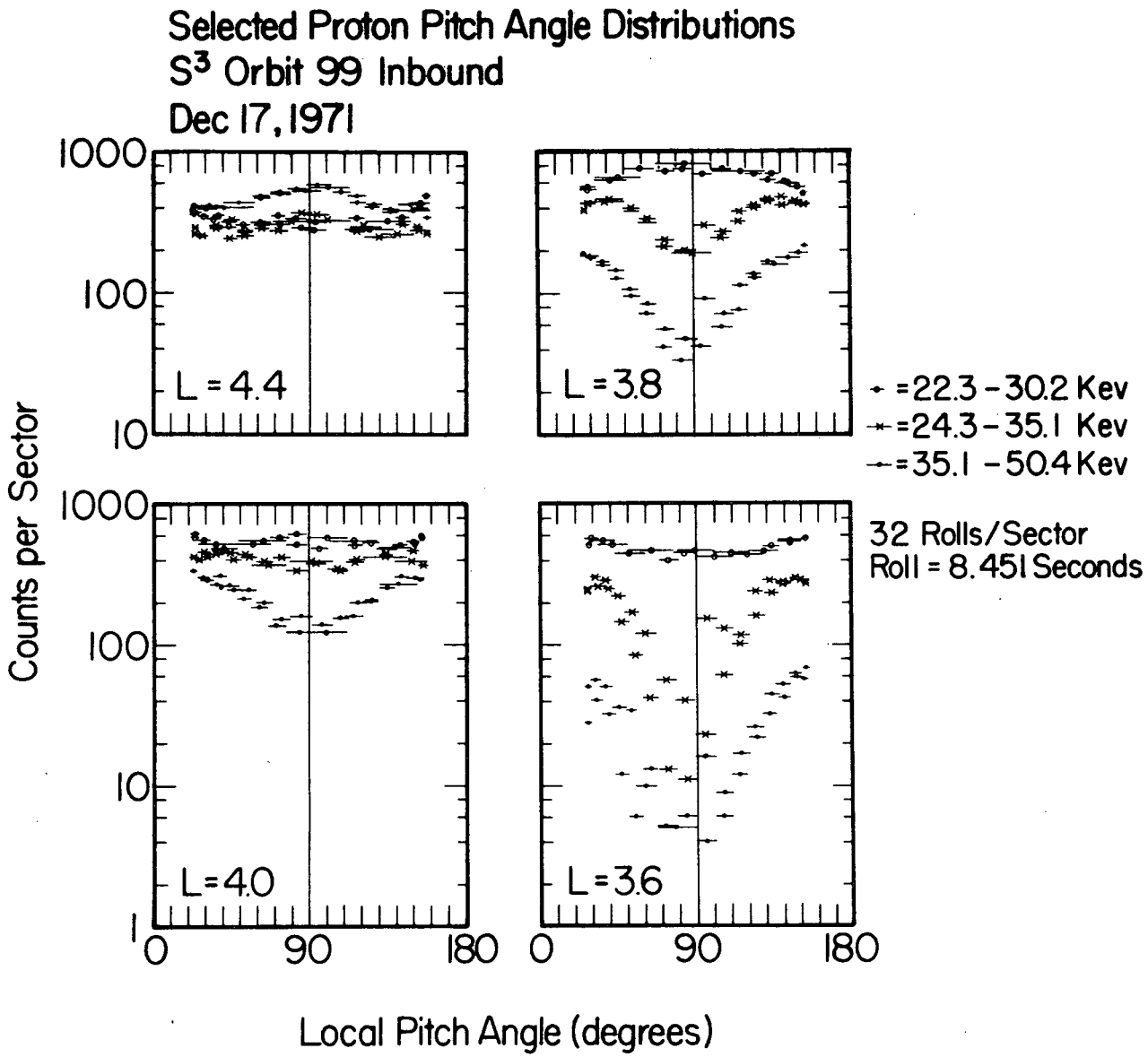

Figure 2. Evolution of proton pitch angle distributions through region of steep gradient, as S^3 was at geomagnetic latitude of ∿12°.

regions are lost preferentially with the result that in the spatial gradient region of the particle distribution, pitch angle distributions at the higher energies show many more particles mirroring at small pitch angles than in the near equatorial regions. The lower energy band begins to display the equatorial minimum in the pitch angle distribution at the lowest altitude shown in figure 2. Note that even though the center energies of the two lowest channels shown in figure 2 are separated by only 4 keV, a sharp difference exists in the evolution of the pitch angle distribution as a function of altitude. This difference we feel is due to two causes: (1) a resonant energy effect and (2) strong energy diffusion.

In figure 3, we present the differential flux values as a function of altitude for $\alpha = 90° \pm 10°$. The two highest differential energy bands display a radial profile which is qualitatively quite similar to radial profiles displayed previously in the literature for integral energies above $\sim$100 keV (Davis and Williamson, 1963; Williams, 1970). However, note that the lower four energies show a markedly different behavior. As the altitude decreases the lower four channels are either at or increase to a maximum flux value and at some lower altitude suddenly decrease in intensity resulting in a steep low altitude intensity gradient. It is also seen that the lower differential energy channels show the intensity decrease at lower altitudes. This is in qualitative agreement

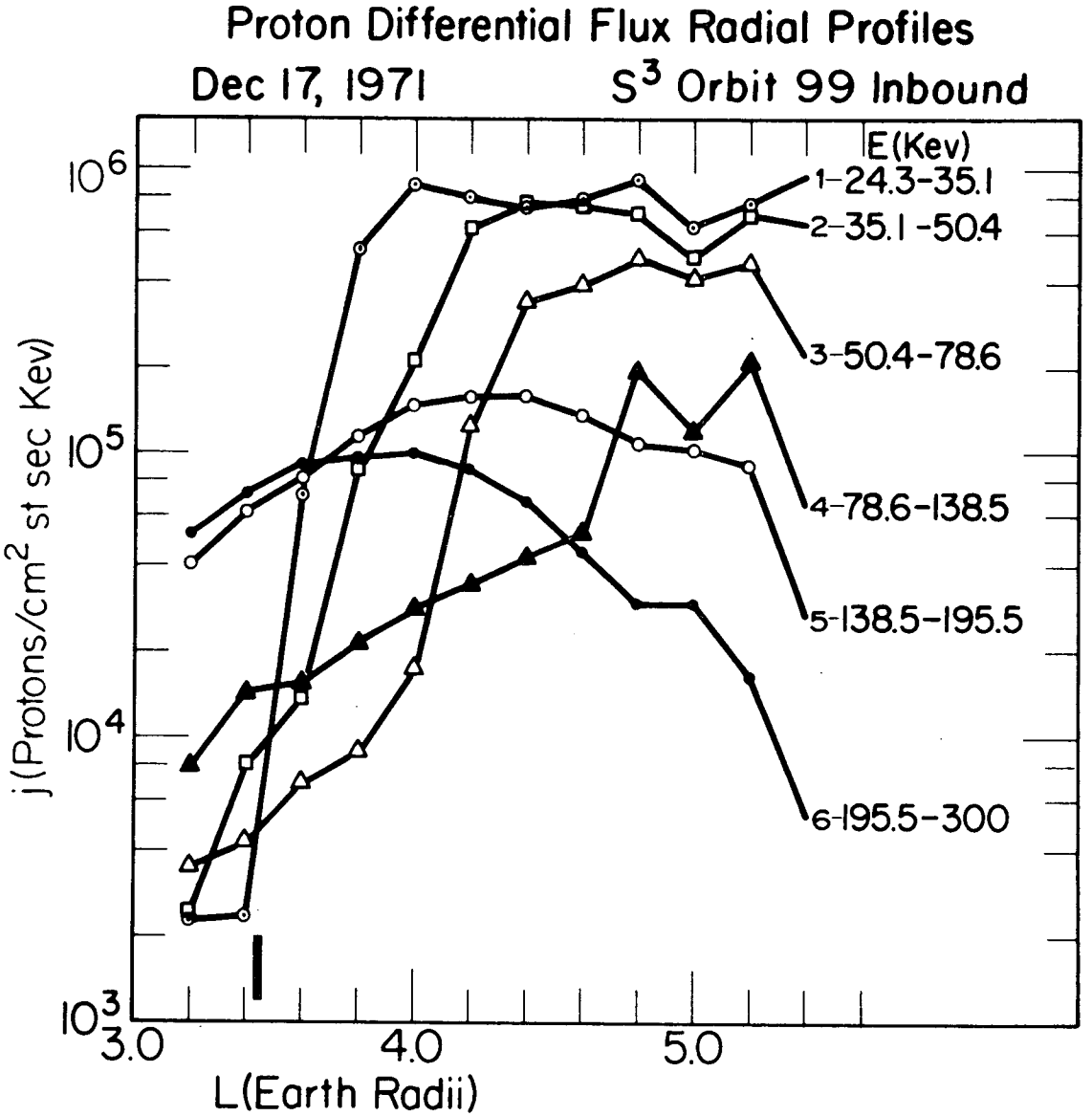

Figure 3. Proton differential flux versus altitude for six energy bands. Vertical bar at L = 3.45, same as in figure 1, α = 90 ±10°.

with the initiation of the ion-cyclotron instability in which the resonant energy is inversely proportional to the total plasma density and would thus decrease as the plasmapause (higher density) is approached (Kennel and Petschek, 1966; Cornwall et al., 1970).

In figure 4, we present the evolution of the proton differential energy spectrum for $\alpha = 90° \pm 10°$ as the region of the spatial gradient is approached. Three points of interest in figure 4 are:

1. The development of a deep trough in the differential energy spectrum;
2. the appearance of a high energy peak in the differential energy spectrum; and
3. a build-up of intensities observed at energies just below the strongly resonant region indicative of significant energy diffusion especially at L = 3.6 and from 10-20 keV.

We wish to present the following discussion arguing that the preceding data are consistent with the initiation of the ion-cyclotron instability which causes the initial decrease in intensities as the region of the radial gradient is approached.

Exponential wave growth is expected if the energetic proton population satisfies the following conditions (Kennel and Petschek, 1966; Cornwall et al., 1970):

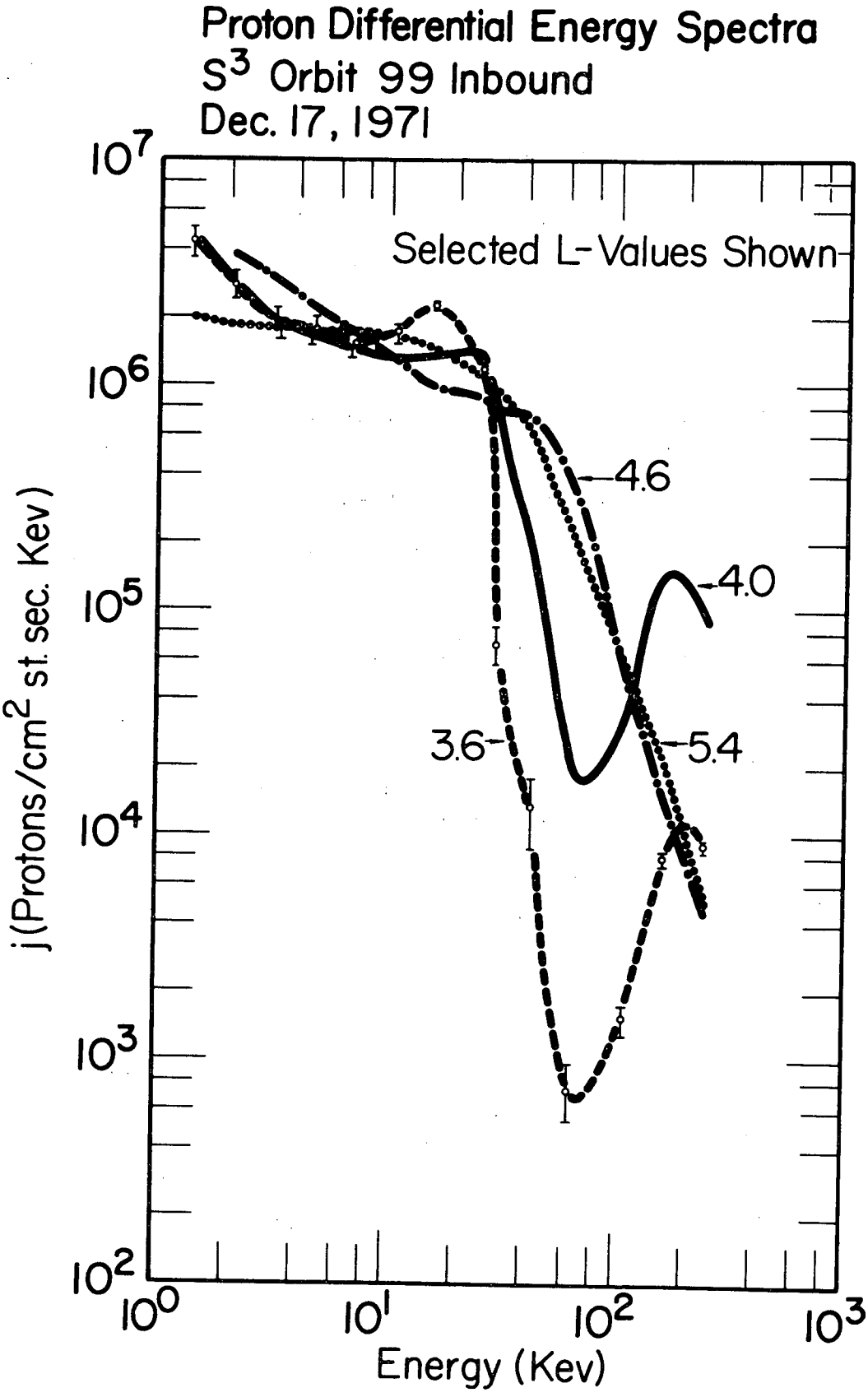

Figure 4. Evolution of proton differential energy spectra through region of steep gradient, α = 90° ±10°.

(1) $$A > \frac{1}{\frac{\Omega}{\omega} - 1}$$

A = a measure of proton pitch angle anisotropy

($A \equiv \frac{n}{2}$ for $\sin^n \alpha$ distribution)

Ω = proton gyrofrequency

ω = wave frequency

(2) $$J_{\text{Max}}(E > E_R) > KL^{-4} \text{ protons/cm}^2\text{sec}$$

L = McIlwain L parameter

E_R = parallel resonant energy

(3) $$E_R > \frac{B^2}{8\pi N}\left(\frac{\Omega}{\omega}\right)^2\left(1 - \frac{\omega}{\Omega}\right)^3$$

or from (1)

$$E_R > \frac{B^2}{8\pi N} A^{-2}(1+A)^{-1}$$

B = magnetic field magnitude

N = total plasma density

Similar criteria hold for the stimulation of such instabilities in the energetic electron population (Kennel and Petschek, 1966) and the effects of the electron branch of the instability (whistler mode interaction) have been discussed in connection with electron precipitation phenomena (Brice, 1970; Brice and Lucas, 1971).

The pitch angle anisotropy identifies at a given point in space the wave frequencies which will resonate with the proton particle distribution. We thus interpret the initiation of the intensity decreases in figure 3 in the following manner. The lower four differential channels show proton fluxes at high altitudes which exceed the limiting flux given in (2). As the altitude decreases, the resonant energy decreases due to an increasing plasma density as the plasmapause is approached. When the resonant energy matches a particular differential energy band, protons in that band suffer an intensity decrease due to the initiation of the ion-cyclotron instability as all conditions are then met. As the altitude continues to decrease (N increasing) this effect is progressively seen through the lower energy channels as displayed in figure 3. The high energy channels do not show similar effects because they do not exceed J_{Max}.

To more quantitatively test this hypothesis, we show in figure 5 omnidirectional flux values versus altitude. Here we have summed through the lowest four energy channels which appear to be in resonance and have shown the higher energy channel by itself which is apparently unaffected. For comparison, we have included a plot of the maximum allowed flux value from (2) for two values of the constant K, 5×10^{10} and 10^{10} $cm^{-2}sec^{-1}$. From figure 5 we see that a critical flux value of $5 \times 10^{10}L^{-4}$ protons/cm^2sec, is consistent with the

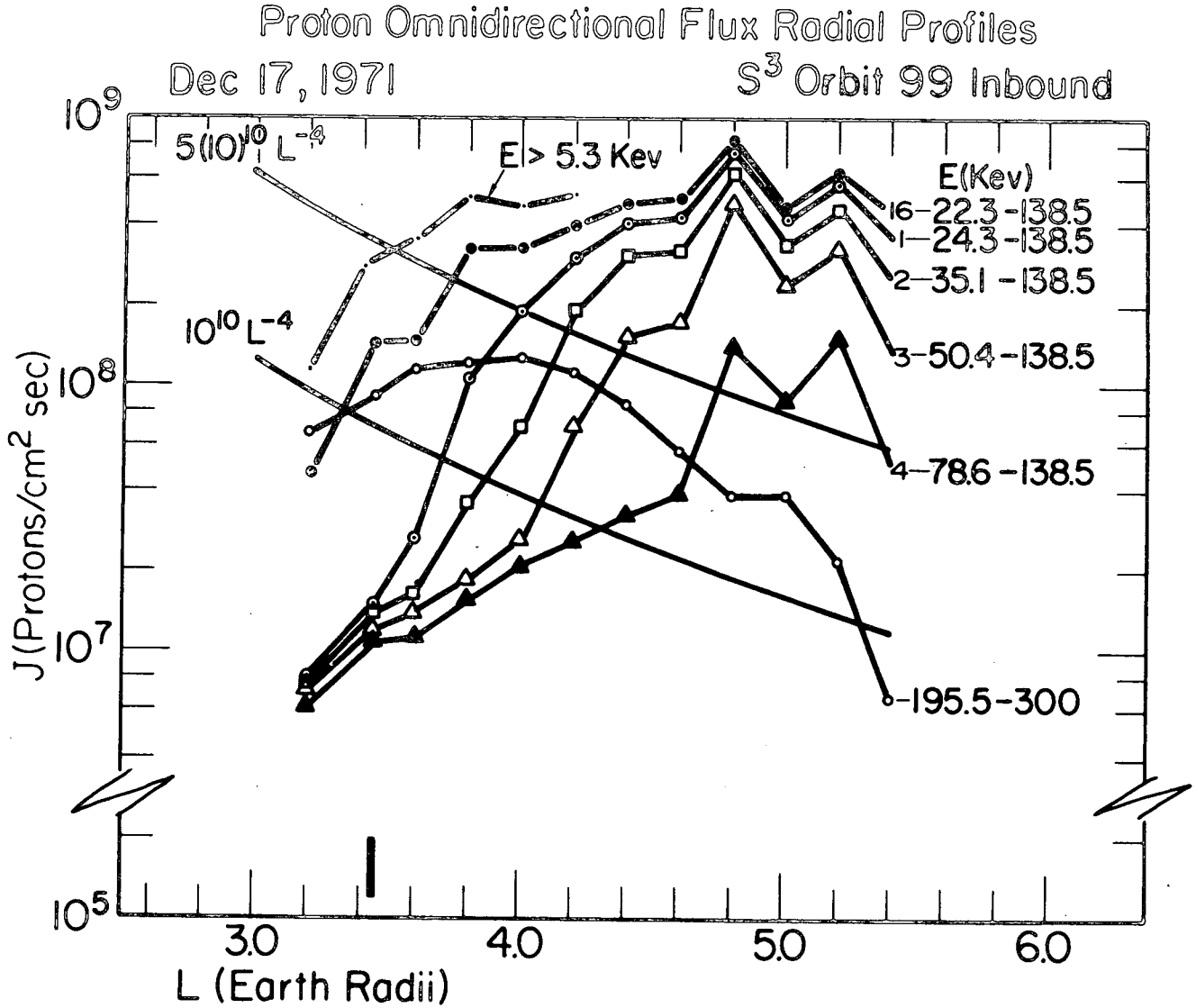

Figure 5. Omnidirectional fluxes versus altitude compared with $J_{max} = KL^{-4}$ for two values of K. Vertical bar at L = 3.45, same as in figure 4, $\alpha = 90° \pm 10°$.

above discussion. Theoretical estimates of K yield a lower limit of $5\text{-}7(10)^{10}$ $cm^{-2}sec^{-1}$ (Kennel and Petschek, 1966; Cornwall, 1966) and recent low altitude experimental normalization of K has given $\sim 1.3(10)^{10} cm^{-2}sec^{-1}$ (Cornwall et al., 1971a).

Utilizing this interpretation we then are able to measure the resonant energy within a certain differential energy band as a function of altitude from figure 3 by obtaining the altitude at which the sudden intensity decrease occurs. We therefore can extract the total plasma density N, as a function of altitude by observations of the resonant energy, E_R, the pitch angle anisotropy, A, and the magnetic field, B. This result is shown in figure 6. The vertical bars are the values of N extracted and reflect the fact that the resonant energy is measured as a differential energy band. A dashed line is drawn through the vertical bars to indicate that a normal plasmapause structure is obtained from the interpretation that the data in figures 3, 4, and 5 are consistent with the initiation of the ion cyclotron instability.

It is possible to explain qualitatively the evolution of pitch angle structures shown in figure 2 by the use of a resonant instability provided that energy diffusion is significant. Excluding the singular point at $\alpha_e = \frac{\pi}{2}$, there are several reasons why the interaction process will be more effective in the near equatorial regions (Kennel and Petschek,

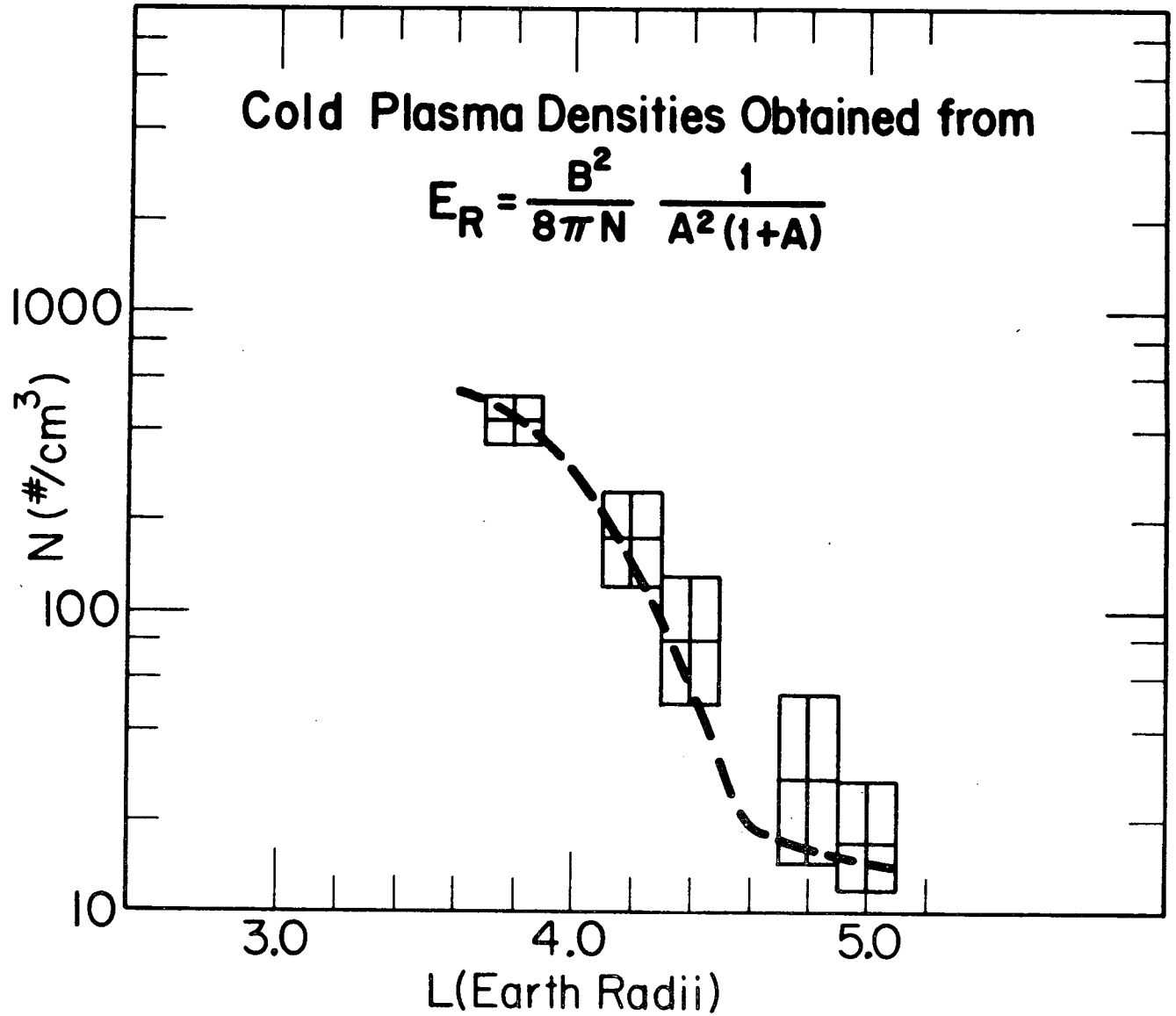

Figure 6. Plasma densities obtained from resonant energy equation with E_R, B, and A measured at or just before point of intensity decrease. N is extracted from equation shown in figure. Vertical range of N due to observation of E_R in particular energy interval. Dotted line simply indicates that a "normal" plasmapause is consistent with the data.

1966). For example, wave growth rate is largest near the equator due to the small B and thus lower resonant energies required. In addition, particles mirroring well off the equator spend less time in the interaction region (have large $v_{||}$ at the equator) and are thus less effectively scattered. Thus while particles are lost from the detecting channel through both pitch angle and energy diffusion at all pitch angles the effect is greater near the equator.

If the above interpretation is correct and protons are put into strong pitch angle diffusion, the intensities shown in figures 3 and 4 represent sufficient energy to cause a mild red arc through the mechanism suggested by Cornwall et al. (1971b). In checking the records of the Fritz Peak Observatory of the NOAA Aeronomy Laboratory, it was found that a mild red arc was observed at the time these observations were made (Hernandez, personal communication). Observations of the red arc occurred at near local midnight and the radial gradient displayed in figure 1 was observed as S^3 passed through the local midnight meridian. Rough estimates have shown that the energy available to the ionosphere from the particles shown in the preceding figures was sufficient to support the intensity of the red arc observed.

For the data presented in this report, ω/Ω is approximately 1/5. At L = 4, this gives an Alfven wave frequency cutoff of approximately 1.6 Hz. In the gradient regions,

$3.4 \leq L \leq 3.6$, enhanced variations in the 1 to 3 Hz channel of the electric field detector were observed (Maynard and Cauffman, 1972). However, no variations were seen above the sensitivity threshold for the 1 to 3 Hz channel of the search coil magnetometer (Parady, personal communication). It is possible that with the intensities involved, the growth rate would be such that wave amplitudes exceeding the search coil magnetometer thresholds would not have occurred.

In summary, we wish to point out that the data presented here are consistent with the initiation of the ion cyclotron instability when the requirements (1), (2), and (3) are met. These requirements are met initially at the altitude at which the sudden intensity decrease occurs (figure 3). However, after the initiation of the instability, we find that the linear theory is outlined by (1), (2), and (3) is unable to explain the further evolution of the intensities, pitch angle distributions and energy spectra of the ring current particles. First, the theory as it now stands has no mechanism whereby energy loss is formally introduced into the scattering mechanism. Thus the pitch angle distribution of figure 2 cannot be satisfactorily explained via ion-cyclotron resonance. Secondly, the present theory also has no mechanism whereby the fluxes would precipitate much below J_{max}. The instability should self-quench and basically return the particle fluxes to or just below J_{max}. However, we see from figures 3, 4,

and 5 that this is not the case and the intensities continue to decrease to one to two orders of magnitude below this critical flux limit. Therefore to describe the actual evolution of the data presented herein, we feel that non-linear effects, additional instabilities, and particle injection and drift as a function of pitch angle (Konradi et al., 1972) must be considered in more detail.

ACKNOWLEDGEMENTS

We wish to acknowledge valuable discussion with D. Evans, W. Bernstein, F. Scarf, R. Fredericks, J. M. Cornwall, G. Haerendel, N. Brice, and C. McIlwain concerning these data. It is a pleasure to recognize the efforts of Mr. J. Winkleman, whose programming efforts have made this analysis possible. We wish to thank R. Hoffman and L. Cahill respectively for discussions regarding proton data $\lesssim$ 25 keV and magnetometer data used in this study. We also wish to acknowledge and thank the S^3 Project Office for their untiring efforts over the six years it required from the initiation of the S^3 program to the launch of the first spacecraft, S^3-A. In particular, we thank Messrs. G. W. Longanecker, F. Carr, K. Sizemore, R. A. Hoffman, and R. Martin. One of us (D.J.W.) wishes to thank NASA, GSFC, for the opportunity of having been associated with the inception, design and development of the S^3 program and for having been allowed to serve as Project Scientist from November 1965 through August 1970. This work was done in part under NASA Contract S-50028.

REFERENCES

Brice, N. (1970), "Artificial enhancement of energetic particle precipitation through cold plasma injection: A technique for seeding substorms?", *J. Geophys. Res.* 75, 4890.

Brice, N., and C. Lucas (1971), "Influence of magnetospheric convection and polar wind on loss of electrons from the outer radiation belt," *J. Geophys. Res.* 76, 900.

Cahill, L. J. Jr. (1972), "Magnetic storm inflation in the evening sector," Preprint, University of Minnesota.

Cornwall, J. M. (1966), "Micropulsations and the outer radiation zone," *J. Geophys. Res.* 71, 2185.

Cornwall, J. M., F. V. Coroniti, and R. M. Thorne (1970), "Turbulent loss of ring current protons," *J. Geophys. Res.* 75, 4699.

Cornwall, J. M., H. H. Hilton, and P. F. Mizera (1971a), "Observations of precipitating protons in the energy range 2.5 keV $\leq$ E $\leq$ 200 keV," *J. Geophys. Res.* 76, 5520.

Cornwall, J. M., F. V. Coroniti, and R. M. Thorne (1971b), "Unified theory of SAR arc formation at the plasmapause," *J. Geophys. Res.* 76, 4428.

Davis, L. R., and J. M. Williamson (1963), "Low energy trapped protons," *Space Res.* 3. 365.

Kennel, C. F., and H. E. Petschek (1966), "Limit on stably trapped particle flux," *J. Geophys. Res.* 71, 1.

Konradi, A., D. J. Williams, and T. A. Fritz (1972), "Energy spectra and pitch angle distributions of storm time and substorm injected protons," Preprint, NASA Manned Spacecraft Center.

Longanecker, G. W., and R. A. Hoffman (1972), "S^3-A (Explorer 45) spacecraft and experiment description," Preprint, NASA Goddard Space Flight Center.

Maynard, N., and D. P. Cauffman (1972), "Double floating probe measurements on S^3-A," Preprint, NASA Goddard Space Flight Center.

Williams, D. J. (1970), "Trapped protons ≥ 100 keV and possible sources," in *Particles and Fields in the Magnetosphere*, B. M. McCormac, ed. (D. Reidel Publishing Co.), 396.